LWT - Food Science and Technology 151 (2021) 112146

Contents lists available at ScienceDirect

LWT

journal homepage: www.elsevier.com/locate/lwt

Evaluation of the addition of artichoke by-products to O/W emulsions for oil microencapsulation by spray drying

Mónica Umaña [a], Paweł Wawrzyniak [b], Carmen Rosselló [a], Beatriz Llavata [c], Susana Simal [a,*]

[a] Department of Chemistry, University of the Balearic Islands, Ctra. Valldemossa, km. 7.5, 07122, Palma de Mallorca, Spain
[b] Faculty of Process and Environmental Engineering, Lodz University of Technology, 213 Wolczanska Str, Lodz, 90-924, Poland
[c] Analysis and Simulation of Agro-food Processes Group, Food Technology Department, Universitat Politècnica de València, Camino de Vera s/n, E46022, Valencia, Spain

ARTICLE INFO

Keywords:
Artichoke by-product
Emulsion
Microencapsulation
Spray drying
Shelf life

ABSTRACT

This study aimed to evaluate the use of artichoke bracts in oil microencapsulation by spray drying. Thus, 1% and 2% w/w of this material was added to sunflower O/W emulsions to partially replace maltodextrin and substitute Tween®20. Emulsions were compared with a control containing only maltodextrin as wall material and Tween®20 as emulsifier. The emulsion containing 2% of artichoke exhibited higher ($p < 0.05$) viscosity and stability against coalescence and flocculation (24 h) and 20% higher encapsulation efficiency after spray drying, compared with control. The three microcapsules showed similar microstructure, density, porosity, flow properties, and Tg. Microcapsules containing artichoke exhibited, on average, 15% larger particles, 19% lower moisture content, and 9% lower solubility, besides perceptible colour changes. Microcapsules containing artichoke (2%) showed lower oxidation indicators content (37%) after spray drying and over 2 months of controlled storage (35 °C, 50% relative humidity) than control. After 90 days, decreases in linoleic acid were observed in all the samples (up to 24%), with increases of oleic and saturated fatty acids. The control showed the highest increase in saturated fatty acids (73%). Hence, artichoke bracts can be exploited for their application in lipid microencapsulation because of their emulsifier properties and the oxidative protection they provide.

1. Introduction

Polyunsaturated fatty acids (PUFAs) are essential for human health and carriers of lipophilic bioactive compounds; however, they are sensitive to oxidation. Two of the most effective strategies for improving lipids stability are the addition of antioxidants and microencapsulation by spray drying to prevent contact with oxygen and other stressors (Timilsena et al., 2017). This process has technological advantages such as easier storage, longer shelf life, easier dilution in small quantities, and others (Ye et al., 2018). Therefore, microencapsulation has been widely applied as a technique for the protection and controlled release of functional food components such as PUFAs, antioxidants, flavors, vitamins, and so on (Gharibzahedi et al., 2018). Microencapsulation usually requires the dispersion of the lipids in O/W emulsions before spray drying. The composition and characteristics of this initial emulsion, such as the wall material type and content, viscosity, droplet size, and stability are decisive for the oil encapsulation efficiency (Carneiro et al., 2013; Linke et al., 2020).

Recently, consumers have come to prefer products free of artificial additives (Berton-Carabin & Schroën, 2019). Hence, there is a constant search for novel natural materials to protect lipophilic active ingredients in the food industry. Thus, the use of natural polysaccharides and proteins as wall materials in the microencapsulation of lipids has gained attention. Pectins, β-glucans, and inulin are some examples of natural polysaccharides already evaluated in lipid microencapsulation (Gallotti et al., 2020; Pieczykolan & Kurek, 2019). Natural proteins such as those from milk, soy, pulses, and cereals have also been investigated (Costa et al., 2015; Fioramonti et al., 2019; Rascón et al., 2011). The combination of carbohydrates and proteins has gained attention since an efficient formation of the dry crust and good lipid oxidative stability have been reported (Le Tan et al., 2017; Locali et al., 2019).

In this context, vegetable by-products, especially those containing polysaccharides and proteins, might be interesting for their application in lipid microencapsulation. Valorization of by-products as renewable raw matters is attracting attention (Faustino et al., 2019). However, very few investigations have been performed evaluating food by-products in lipid microencapsulation (Marson et al., 2020; Nasri et al., 2020). The

* Corresponding author. Ctra Valldemossa km 7.5, 07122, University of the Balearic Islands, Palma de Mallorca, Spain.
E-mail address: susana.simal@uib.es (S. Simal).

https://doi.org/10.1016/j.lwt.2021.112146
Received 1 February 2021; Received in revised form 15 June 2021; Accepted 13 July 2021
Available online 14 July 2021
0023-6438/© 2021 The Authors. Published by Elsevier Ltd. This is an open access article under the CC BY-NC-ND license (http://creativecommons.org/licenses/by-nc-nd/4.0/).

Abbreviation

a*	CIELab coordinate (redness/greenness)
AA	Antioxidant activity (g gallic acid equivalent/100 g dm)
AB	Artichoke bracts flour
b*	CIELab coordinate (yellowness/blueness)
CCI	Carr's compressibility index
CI	Creaming index
d_{50}	Median diameter (μm)
DE	dextrose equivalent
dm	Dry matter
DSC	Differential scanning calorimetry
dTGA	Derivate of thermogravimetric analysis
FAME	Fatty acids methyl esters
GAE	Gallic acid equivalent
HR	Hausner ratio
L*	CIELab coordinate (Luminosity)
MD	Maltodextrin
PUFAs	Polyunsaturated fatty acids
RH	Relative humidity (%)
SA	Specific absorbance of conjugated dienes at 234 nm
SEM	Scanning electron microscopy
TE	Trolox equivalent
Tg	Glass transition temperature
TGA	Thermogravimetric analysis
Wg	Oil mass in volume of organic solvent (g/100 mL)
ΔE	Total color change
ρ	True density (kg/m^3)
ρb	Bulk density (kg/m^3)
ρt	Tap density (kg/m^3)

use of any innovative material in the microencapsulation process needs to be assess. For instance, it is necessary to evaluate the effect of these novel materials on the characteristics of the O/W emulsions and on the properties of the final microcapsules, especially on the encapsulation efficiency and the oxidative stability of the encapsulated oil.

Among the agri-food by-products, it is remarkable the case of artichoke bracts since they represent ~60% of the weight of the whole vegetable (Ruiz-Aceituno et al., 2016) and are rich in polysaccharides including insoluble (cellulose) and soluble dietary fibre (inulin) (Villanueva-Suárez et al., 2019). Insoluble polysaccharides from plants have been used as solid particles to stabilize Pickering O/W emulsions, showing outstanding stability against coalescence (He et al., 2020; Huc-Mathis et al., 2021). The presence of inulin is interesting since it is a prebiotic fructooligosaccharide (Villanueva-Suárez et al., 2019) with technological properties such as emulsion stabilizer (Franck, 2002). Artichoke bracts also contain proteins (Almela et al., 2005) and antioxidants such as phenolic acids (Pandino et al., 2011). The presence of antioxidants would be useful for the protection against the oxidation of the encapsulated oil.

The aim of this work was, therefore, to evaluate the usefulness of artichoke bracts in oil microencapsulation by spray drying. We hypothesize that the addition of this material would stabilize O/W emulsions and improve the oil oxidative stability. Hence, two emulsions were prepared and spray-dried containing 1 and 2% w/w of artichoke bracts, using sunflower oil as a model lipophilic compound. These emulsions and microcapsules were compared with a control with a conventional composition for spray drying (only maltodextrin as wall material and 0.14% w/w Tween®20 as emulsifier).

2. Materials and methods

2.1. Chemical reagents

Sorbitan monolaurate (Tween®20) and maltodextrin DE 17–19 (MD) were purchased from PanReac AppliChem (Spain). Hexane (extra pure), isopropanol (extra pure), petroleum ether (boiling point 40–60 °C, reagent grade), methanol (HPLC grade), ethanol (extra pure), and acetonitrile (HPLC grade) were obtained from Scharlau (Spain) and toluene (analytical grade) from Labkem (Spain). Standard of chlorogenic acid (≥95%) was purchased from Sigma-Aldrich (Spain).

2.2. Raw matter

Artichokes (*Cynara Scolimus*) were purchased in a local market in Palma de Mallorca (Spain). The bracts were separated, freeze-dried (Telstar LyoQuest, Spain) at −50 °C and vacuum pressure of 30 Pa, ground (ZM 200– Retsch®, Germany), and sieved to a particle size <0.09 mm (FIT–0200, Filtra, Spain). This flour from artichoke bracts was named AB.

The AB moisture content was determined using the AOAC method 934.06 (AOAC, 1997). Protein, lipid, and ash content were determined as described by Umaña et al. (2020). The total carbohydrate content was estimated as the difference to 100 of the sum of protein, lipids, and ash content. The fibre content was estimated by obtaining the alcohol insoluble residues (Eim et al., 2008), and characterized by releasing neutral monosaccharides by Saeman hydrolysis and transforming them into alditols before gas-liquid chromatography (GC) analysis followed as described by Umaña et al. (2020). Uronic acids were determined by colourimetry (Coimbra et al., 1996). Inulin was determined using the method proposed by Saengkanuk et al. (2011).

The total phenolic compounds were extracted in methanol as described by Vallespir et al. (2019) and determined using the Folin-Ciocalteu assay. The antioxidant activity (AA) was measured using the FRAP, CUPRAC, and ABTS assays (Vallespir et al., 2019). The results were expressed as g of gallic acid equivalent (GAE)/100 g dry matter (dm) in the case of the total phenolic compounds and as g of Trolox equivalent (TE)/100 g dm in the case of the AA. From the methanolic extract, the chlorogenic acid content was measured as described by Wang et al. (2003) with small modifications by HPLC using an Atlantis dC18 column (3 μm; 3,9 × 150 mm) (Waters, USA). The mobile phases were water with 0.2% phosphoric acid (A) and acetonitrile (B) using the following gradient: initial 6% B, linear gradient to 30% B in 20 min, with a flow rate of 1 mL/min and temperature of 25 °C. The detection wavelength was 330 nm. The identification and quantification were performed using calibration with a standard.

Sunflower oil was used as a model for lipophilic compounds because of its high PUFAs content (~60%) (Multari et al., 2019). It was purchased from a local store (Palma de Mallorca, Spain) and purified to remove the endogenous antioxidant following the stripping method described by Hernández Sanchez, Cuvelier, and Turchiuli (2015).

2.3. Emulsions preparation

Three O/W emulsions (C (control), AB1, and AB2) were prepared

Table 1
Composition (g/100 g emulsion) of the O/W: control (C), and those containing artichoke bracts flour: AB1 and AB2.

COMPONENT	C	AB1	AB2
Water	60.00	60.00	60.00
Maltodextrin	35.86	35.00	34.00
Oil	4.00	4.00	4.00
Artichoke bracts flour (AB)		1.00	2.00
Tween®20	0.14		

with the composition shown in Table 1. The C emulsion was prepared following the protocol described by Hernández et al. (2015) with some modifications. First, the MD was dissolved in 85% of the water required according to the formulation shown in Table 1. Secondly, an O/W emulsion was prepared with the rest of the water (15%) and with Tween®20, using an Ultra-Turrax© (T25 Digital, IKA, Germany) at 1821 g for 15 min. Finally, this emulsion was mixed with the aqueous solution of MD previously prepared.

Regarding the emulsions containing AB, MD was dissolved in water and then AB was dispersed with an Ultra-Turrax© at 1821 g (8 min). Thereafter, the oil was added mixing for 15 min at 1821 g. The samples (C, AB1, and AB2) were kept in an ice-water bath maintaining the temperature under 40 °C when using the Ultra-Turrax©.

2.4. Emulsions characteristics

Apparent viscosity of emulsions was measured with a J. P Selecta rotational viscometer (ST-DIGIT R, Spain) at 25 °C with a shear rate (γ) of 53 s^{-1}.

The droplet size distribution of the emulsions was determined using an Olympus BX60 microscope (Optical Co. Ltd., Japan) connected to a camera (Moticam 3, Spain). The emulsions were diluted in distilled water (3:20 v/v) and immediately observed with a 20x objective. Micrographs (minimum 5 per sample, ~30000 droplets) were processed with ImageJ 1.52a software (Rasband, 2020), the photos were transformed into the 8-bit and contrast was enhanced (5% normalized). Thereafter, the functions "make binary" (Hosseini et al., 2015) and "watershed" were applied to construct a boundary for each droplet (Schuster et al., 2012). The area of each droplet was obtained automatically using a scale. The droplets' volume and diameter were calculated from the area assuming the particles were spherical. The micrographs with floccules were submitted to further analysis to estimate the % flocculated oil volume. Thus, after transforming the micrograph to 8-bit and binary, the "minimum filter" was applied (radius 1 pixel) to discard droplets that were not into floccules. Thereafter, the function "find maxima" (noise tolerance: 10, output type: "segmented particles") was applied. Finally, the functions "dilate" and "find edges" were used, and the area of each particle was measured. The droplet size distribution was measured immediately after the emulsion preparation and several times over 24 h. Meanwhile, the emulsions were stored at 4 °C in containers with a capacity of 100 mL (55 × 70 mm). The creaming index (CI) of the emulsions was measured as described by Edris et al. (2016) at several times for 24 h maintaining the sample at ~22 °C.

2.5. Spray drying of the emulsions

Emulsions were spray dried in a Buchi B-290 spray dryer (Buchi, Switzerland) at 175 °C inlet temperature, 32 m^3/h (80%) of aspiration, 8.3 mL/min (25%) of pumping of the emulsions and an atomization air flow rate of ~0.83 m^3/h. A two-fluid nozzle atomizer with an opening of 0.7 mm was used and the nuzzle cleaner was set to 12 strikes/min. The outlet temperature was 100–102 °C. These parameters were determined from preliminary experiments to obtain a dried powder with a low moisture content (<3 g/100 g dm) (results not shown). Emulsions were magnetically agitated during the drying process. Each emulsion was prepared and dried in duplicate.

2.6. Microcapsules characteristics

The powders were observed by scanning electron microscopy (SEM). Samples were mounted on aluminium stubs with double-sided sticky carbon tape and subjected to gold sputter coating. A microscope HITACHI S–3400N (Germany) accelerated at 15 kV and under vacuum pressure of 40 Pa was used. The micrographs were analyzed (minimum 8 photos per sample, ~4000 particles) as described in section 2.4. The dried emulsions were reconstituted in water (2 g of powder in 3 mL of distilled water at 50 °C) and the size of the droplets was analyzed as described in section 2.4.

The encapsulation efficiency was measured by quantifying the surface and the total oil, the oil in the core was the difference between them. Surface oil extraction was carried out according to the GEA Niro Method No. A 10a (2005). The total oil was determined as described by Kim et al. (2005). Emulsions were reconstituted (1 g of powder and 2 mL of distilled water at 50 °C) and oil was extracted with 50 mL hexane/iso-propanol (3:1 v/v). Encapsulation efficiency was expressed as the mass of oil in the core/total mass of oil %.

The moisture content was determined using the method 934.06 (AOAC, 1997), and the water activity (aw) was measured at 25 °C using a NOVASINA thermoconstanter TH200 (Switzerland).

The powders' hygroscopicity was determined as described by Zotarelli et al. (2017) at 25 °C, 75.3% relative humidity (RH) for 7 days. The solubility of the microcapsules and AB was measured according to Pieczykolan and Kurek (2019). The colour was measured with a CM-5 colourimeter (Konica Minolta, Japan) (Vallespir et al., 2018) and expressed using the CIELab* coordinates: L* (luminosity), a* (redness/greenness), and b* (yellowness/blueness). The total colour change (ΔE) was calculated by comparing the powders containing AB with C, and microcapsules with their wall materials (Eq. (1)).

$$\Delta E = \sqrt{\Delta L^{*2} + \Delta a^{*2} + \Delta b^{*2}} \quad (1)$$

The bulk (ρ_b), tapped (ρ_t) and true density (ρ) were determined as described by Premi and Sharma (2017). The porosity (Eq. (2)) and the flow properties in terms of Hausner ratio (HR) (Eq. (3)) and Carr's compressibility index (CCI) (Eq. (4)) (Tze et al., 2012) were calculated as follows:

$$Porosity = 1 - \rho_t/\rho \quad (2)$$

$$HR = \rho_t/\rho_b \quad (3)$$

$$CCI = (\rho_t - \rho_b)/\rho_t .100 \quad (4)$$

The thermogravimetric analysis (TGA) was carried out with a TA Instruments DMA Q800 (TA Instruments, USA), placing the sample in an aluminium pan into a furnace and heating it from 20 °C to 600 °C (rate of 20 °C/min), with a nitrogen flow of 50 mL/min and recording the sample weight (Umaña et al., 2021). The differential scanning calorimetry analysis (DSC) was performed with a DSC (Mettler Toledo, DSC 3, USA). Samples were heated from −20 °C to 100 °C, in the first heating, 100 °C to −20 °C in cooling, and −20 °C to 150 °C in the second heating (rate 10 °C/min). The glass transition temperature (Tg) was obtained from the DSC thermograms of the second heating (Umaña et al., 2021).

2.7. Oxidative stability

About 35 g of each powder was poured into a vessel inside a hermetic jar placed in a climatic chamber at 35 °C and 50% RH for 90 days. Regular sampling was done at different times and the analysis of dienes performed immediately. The powders were manually homogenized before sampling and randomly changed position after sampling.

The specific absorbance (SA) of dienes was determined as an indicator of primary oxidation products. This determination was carried out in the stripped sunflower oil by diluting it in hexane/iso-propanol (3:1 v/v) and measuring the absorbance at 234 nm. To determine the SA of the oil of the microcapsules, the emulsion was reconstituted in water and the oil was extracted in an organic solvent (hexane/iso-propanol (3:1 v/v)) as described by Hernández et al. (2016). The organic phase containing the oil was separated by centrifugation and an aliquot was diluted to measure the absorbance at 234 nm and the SA was calculated (Eq. (5)).

$$SA = Abs\ 234\ nm/_{Wg} \quad (5)$$

Wg, the oil mass (g) in 100 mL of the solvent solution, was estimated from the total oil content of each powder measured as described in section 2.7 (Kim et al., 2005) assuming that 100% of the oil was extracted.

The fatty acid composition was obtained in the stripped sunflower oil by diluting it in heptane before *trans*-esterification. It was also measured in the encapsulated oil after spray drying and after 90 days of storage. Thus, the oil was extracted from powders as described in this section but using heptane instead of hexane/iso-propanol. Thereafter, the *trans*-esterification with methanolic KOH was performed (AOCS, 2006). Samples were injected in a GC system (Hewlett Packard 5890A, Germany) equipped with a flame ionization detector and a capillary column (SP™-2330, Supelco Inc., USA). The GC analysis was carried out using the conditions described by Rodríguez et al. (2014). The fatty acids methyl esters (FAMEs) were identified by comparing their retention times with those of a commercial standard of FAMEs (Supelco Inc., USA), and results were expressed as the percentage of total fatty acids.

2.8. Statistical analysis

Results were reported as an average of at least three replicates ± standard deviation. Statistical analyses were carried out with R 3.1.0 software (R Core Team, 2017b). Independent means were evaluated with the parametric ANOVA test and Tukey's test to determine the existence of significant differences ($p < 0.05$) (de Mendiburu, 2016; R Core Team, 2017a).

3. Results and discussion

3.1. Characteristics of AB

The composition and other characteristics of AB are shown in Table 2. Carbohydrates were the main component, followed by proteins and ashes, and a small amount of lipid. The proteins content is relatively high considering it is a vegetable (Almela et al., 2005).

Table 2
Composition of the artichoke bracts flour (AB). CIELab* colour coordinates have not units.

Parameter			
Moisture (g/100 g dm)	3.57	±	0.10
Protein (g/100 g dm)	14.88	±	0.93
Lipid (g/100 g dm)	1.24	±	0.10
Ashes (g/100 g dm)	5.40	±	0.01
Total carbohydrate (g/100 g dm)	78.47	±	0.55
Fibre (g/100 g dm)	66.59	±	0.60
Fibre monosaccharides (g/100 g dm)			
Rhamnose	0.44	±	0.02
Fucuse	0.05	±	0.01
Arabinose	1.43	±	0.22
Xylose	12.56	±	1.05
Mannose	0.66	±	0.14
Galactose	0.87	±	0.13
Glucose	25.82	±	0.96
Uronic acids	5.87	±	0.59
Inulin (g/100 g dm)	15.05	±	1.70
Total phenolic content (g GAE/100 g dm)	3.30	±	0.25
Chlorogenic acid (g/100 g dm)	1.46	±	0.07
Antioxidant activity (g TE/100 g dm)			
FRAP assay	8.23	±	0.84
CUPRAC assay	5.98	±	0.79
ABTS assay	5.12	±	0.47
CIELab* colour coordinates			
L*	77.67	±	0.13
a*	−6.01	±	0.03
b*	26.12	±	1.60
Solubility (%)	43.04	±	0.42
Tg (°C)	79.64	±	2.29

An average of at least three replicates is reported.

AB contained a high amount of fibre, meaning a considerable content in polysaccharides. Glucose was the most abundant monosaccharide in the fibre which coincides with the results of Villanueva-Suárez et al. (2019). These authors observed that most of the glucose corresponds to cellulose, which along with some insoluble hemicelluloses, form the insoluble dietary fibre of artichoke bracts. Xylose was the second most abundant monosaccharides of AB, confirming a high presence of hemicelluloses such as xylans and xyloglucans. On the other hand, the soluble fibre would be mainly conformed by inulin and pectins (Domingo et al., 2019). This explains the presence of uronic acid (galacturonic acid is the main pectic monomer), which is the third most abundant monosaccharide of AB. The content of inulin was similar to that reported by Zeaiter et al. (2019) (16.0 ± 1.8 g/100 g dm). According to Villanueva-Suárez et al. (2019), ~28% of the fibre of artichoke bracts correspond to soluble dietary fibre. This value would be ~19 g/100 g dm for AB.

The phenolic compounds content in AB was high and similar to that previously reported (2.5–3.3 g GAE/100 g dm) (Mena-García et al., 2020; Ruiz-Cano et al., 2014). The chlorogenic acid content was similar to that reported by Mena-García et al. (2020) (1.3 g/100 g dm). AB exhibited high AA according to the ABTS, FRAP, and CUPRAC assays.

3.2. Emulsions characteristics

The apparent viscosity of C at 25 °C ($\gamma = 53\ s^{-1}$) was 76 ± 1 mPa s. This figure significantly ($p < 0.05$) increased up to 106 ± 3 and 124 ± 1 mPa s for AB1 and AB2. Given the composition of AB (Table 2), fibre would represent ~0.7–1.3% in AB1 and AB2 emulsions. Plant fibre in these percentages has been found to significantly increases emulsion viscosity (Qi et al., 2020; Zhu et al., 2020). Higher concentrations resulted in emulsions being too viscous, difficult to operate in spray drying according to our preliminary experiments (results not shown).

Fig. 1 shows the oil droplet size distribution of emulsions over time. The percentiles d_{10}, d_{50}, and d_{90} and the span of the droplet size distribution of the initial emulsions (0 h) and the emulsions after 24 h of their preparation are shown in Fig. 2. No significant differences ($p < 0.05$) were observed among the median diameters (d_{50}) of the emulsions (average 2.69 ± 0.10 μm). According to Gharsallaoui et al. (2007), the three emulsions presented droplets with diameters suitable for spray drying (within 1–100 μm). However, AB1 exhibited a small peak on the right, indicating the presence of larger droplets (~12 μm) than in the rest of the emulsions (Fig. 1).

No change was observed in the droplet size distribution of C (Fig. 1) from 0 to 8 h. Nevertheless, the curve shifted to the right after 24 h, significantly ($p < 0.05$) increasing d_{50} (Fig. 2). The distribution of AB1 (Fig. 1), slightly shifted to the right over time, the shoulder observed on the right of the initial distribution moved to ~18 μm after 24 h. However, AB1 did not show significant ($p > 0.05$) increases in any of the percentiles (Fig. 2). Practically no differences were observed in AB2 droplet size distributions over time (Fig. 1), only a small shoulder was observed (~11 μm) after 24 h. No differences ($p > 0.05$) were observed in the percentiles (Fig. 2) of AB2.

Fig. 3 shows micrographs of the emulsions at time 0 and 24 h. At time 0 h, small and uniform droplets were observed in C. According to the image analysis, ~13% of oil volume was flocculated in AB1 at 0 h but only 5% in AB2. Larger droplets were observed in C after 24 h, meaning that coalescence took place. In the case of AB1, even when d_{50} did not significantly increase after 24 h, the flocculated oil increased up to 26%. Emulsion AB2 did not present any coalescence, only a slight increase to 7% of flocculated oil was observed after 24 h.

Overall, the increase of AB concentration improved the emulsion stability against coalescence and flocculation, this could be attributed to more than one mechanism. First, the viscosity increase promoted by this material could have hindered the droplets mobility (Stokes Law). The soluble polysaccharides present in AB, such as inulin and pectins have been found to stabilize emulsions through steric hindrance (Qi et al.,

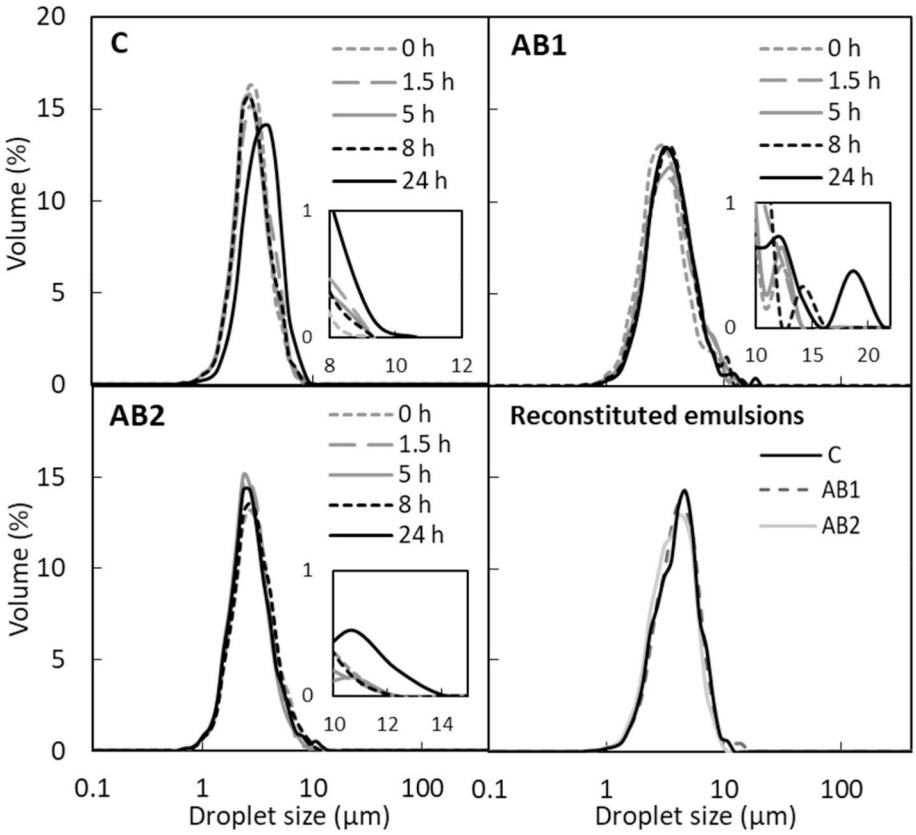

Fig. 1. Droplet size distribution over time of control (C), AB1, and AB2 emulsions. On the right of each chart is an amplification of the zone with the largest droplets of the curves. And droplet size distribution C, AB1, and AB2 reconstituted emulsions.

2020; Xu et al., 2020). Moreover, AB contained proteins that have an amphiphilic nature that enables the molecule to adsorb in the oil-water interface (Can Karaca et al., 2015). Finally, AB solubility was ~43% (Table 2) meaning that most of this material was in form of solid particles in the emulsions (a micrograph of AB particles is shown in Supplementary 1). The non-soluble material would correspond mainly to insoluble fibre that represents ~72% of the total fibre of artichoke bracts according to Villanueva-Suárez et al. (2019). It has been observed that emulsions stabilized by solid particles (Pickering emulsion) show high stability against coalescence due to the irreversible adsorption of these particles at the oil-water interface (Low et al., 2020). Similarly, Qi et al. (2020) prepared O/W emulsions using citrus fibre (17% soluble fibre and 74% insoluble fibre) and concluded that this material stabilized the emulsions through a combination of Pickering effect and the formation of a three-dimensional network of fibre. However, AB1 was highly flocculated, probably because of the insufficient concentration of AB polymers which possibly caused bridging flocculation (Jenkins & Snowden, 1996), and no enough presence of solid particles to perform a Pickering effect.

No creaming was observed in C after 24 h. Meanwhile, ~38% CI was observed in AB1 after 2.5 h and continued increasing to 53% after 24 h. AB2 was initially stable but 14% CI was observed after 24 h. The rapid creaming observed in AB1 can be explained by the high presence of floccules. Floccules move faster upward than individual droplets because of their greater effective size (Dickinson, 2009). Increasing AB concentration resulted in fewer floccules and lower CI. However, AB2 presented more creaming than C even when it was more stable against droplet size variation. Droplets that migrates to the top do not necessarily coalesce and can be redispersed by gentle shaking as we did before the droplet size analysis (section 2.4) (Dodds et al., 2005). Similarly, Massel et al. (2021) prepared W/O/W emulsions with pectins and did not observe droplet size variation for over a month, even when visible creaming was observed after a few days.

3.3. Microcapsules characteristics

Fig. 4 shows micrographs of the microcapsules. The surface and shape did not differ among the microcapsules, independently of their AB content. Both spherical and irregular shaped particles were found with dents. The surface was broadly smooth, but some wrinkled particles were observed. Particles obtained with maltodextrin are usually spherical with a smooth surface (Mohammed et al., 2020). Ré (1998) stated that imperfection such as dents could be a result of a slow process of film formation during drying. There was a small number of hollow particles and very few with holes in the three powders. The presence of hollow particles is common in spray drying and could be due to the inflation of the crust during the final stage of the drying process (Carneiro et al., 2013).

The particle size distribution of the microcapsules is shown in Fig. 5 and the percentiles in Table 3. Particles from emulsions containing AB were significantly ($p < 0.05$) larger than those obtained from C. No significant ($p > 0.05$) differences were observed between the percentiles of AB1 and AB2. The larger particles in powders containing AB could be due to the higher emulsions' viscosity (section 3.2), since an increase in this parameter usually leads to larger droplets during atomization and therefore, bigger dry particles (Tonon et al., 2011). The presence of solid particles in the initial emulsion could also affect the particle size of the final powders. It has been estimated by Whitby et al. (2017) that increasing solid particles proportion results in thicker solid shells covering the oil droplets, this might result in larger particles.

Regarding the reconstituted emulsions, their droplet size distributions are shown in Fig. 1 and their micrographs in Fig. 3. All the emulsions showed an increase in the droplets' size after spray drying, thus, d_{50} increased by 47, 27 and 33% in C, AB1, and AB2. Further, AB1

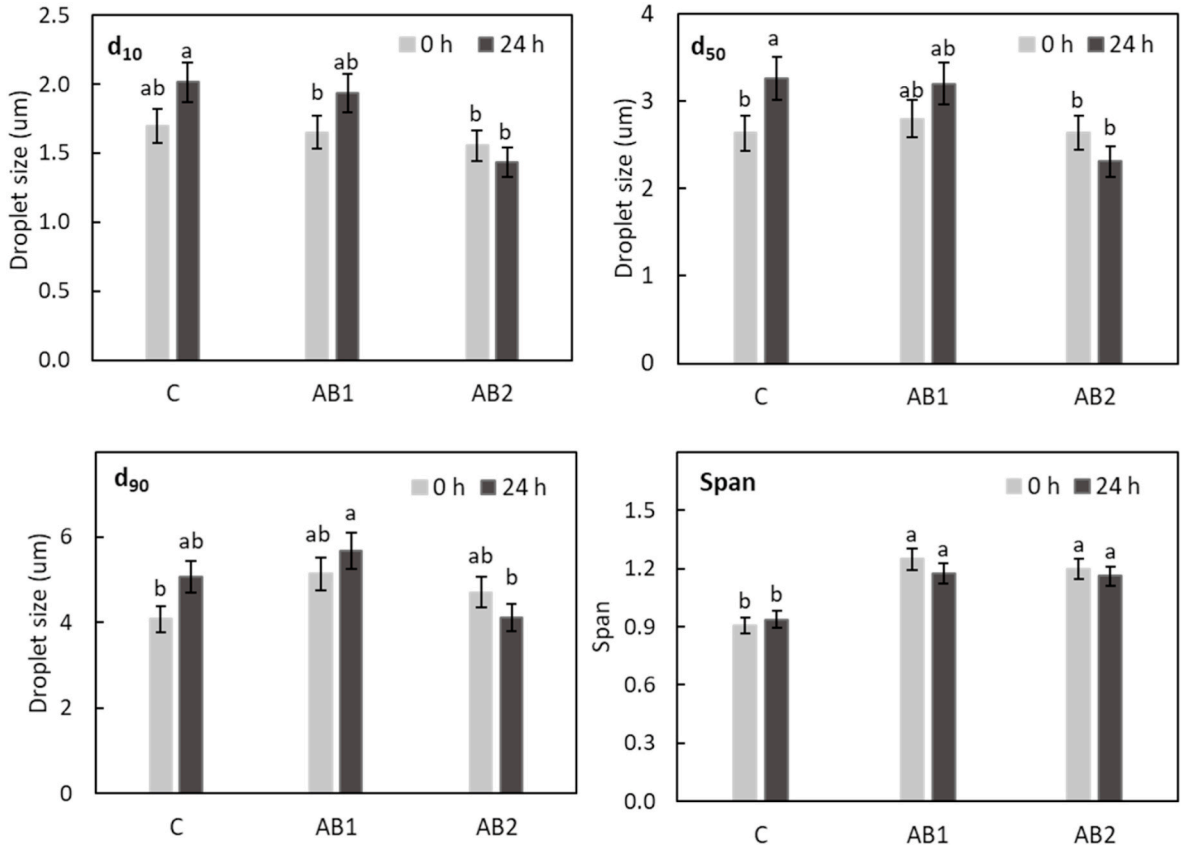

Fig. 2. Percentiles d_{10}, d_{50}, and d_{90} and span at time 0 h and 24 h for emulsions control (C), AB1, and AB2. Different letters on the top of the bars of the same percentile or span indicate significant ($p < 0.05$) differences among the samples.

reconstituted emulsion showed a larger amount of flocculated oil (22% oil) than the initial emulsion. No differences were observed in the amount of flocculated oil in AB2 after spray drying. According to Drusch (2007), larger droplets in reconstituted emulsions can be due to the easy mobility of the droplets during the formation of the solid structure when spray drying, which results in coalescence. This probably occurred in C which has the lowest viscosity enabling the mobility of the droplets. Gharsallaoui et al. (2010) stated that when O/W emulsions containing proteins are heated, the adsorbed proteins could be heat-denatured, and emulsions become susceptible to flocculation and coalescence. AB compounds, such as proteins, possibly suffer physicochemical changes during spray drying, decreasing the emulsion stability.

The encapsulation efficiency (Table 3) was significantly ($p < 0.05$) higher in AB2 (~79%) than in C and AB1. The presence of lipids in AB was not considered for the calculation of the encapsulation efficiency since it was too small to significantly affect this parameter (AB lipids were ~0.03 and 0.06 g/100 powder for AB1 and AB2 respectively). Carneiro et al. (2013) encapsulated flaxseed oil using different wall materials and reported that the lowest encapsulation efficiency corresponded to the least stable emulsion. The AB2 emulsion exhibited the highest stability against coalescence and the best encapsulation efficiency. Di Giorgio et al. (2019), who encapsulated fish oil in soybean protein, observed higher efficiency (58–88%) when increasing the protein content of the initial emulsions; and stated that higher protein content reduces the time needed to form an impermeable crust. The heterogeneous composition of AB seemed to improve the encapsulation efficiency of the oil, however, AB1 was probably too flocculated to enhance it.

The moisture content and the aw (Table 3) were significantly ($p < 0.05$) lower in AB1 and AB2 than in C. The hygroscopicity did not significantly ($p > 0.05$) differ among the samples. According to Ng and Sulaiman (2018), this powders could be considered non-hygroscopic (hygroscopicity <15% at RH 75%). The solubility of the powders was significantly ($p < 0.05$) affected by the addition of AB, probably because of the relatively low solubility of this material (Table 2).

The colour parameters (Table 3) of C remained similar to those of MD ($L^* = 98.10 \pm 0.33$, $a^* = 0.07 \pm 0.02$, and $b^* = 0.79 \pm 0.11$). However, this parameter was affected by the addition of AB. According to Gaurav (2003), values of ΔE higher than 2.3 correspond to changes noticeable to the human eye, therefore, the colour of both AB1 and AB2 was appreciably different from C colour (Table 3). AB colour was green (Table 2), while the powders obtained with AB were light brown. Thus, the ΔEs obtained between AB and AB1 and AB2 were 15 and 12, respectively. Considering AB composition, Maillard browning reactions probably occurred between carbohydrates and proteins during spray drying.

The powders did not show significant differences ($p > 0.05$) in bulk, tapped, and true densities, and neither in the porosity values (Table 3). Powders could be classified as "free-flowing powders" and as "powders with excellent flowability" according to HR and CCI respectively (Tze et al., 2012).

The TGA curves of MD and AB are shown in Fig. 6A. For AB, the first stage of weight loss (~8%) was ~25–100 °C, meanwhile MD exhibited a weight loss of ~6% within the same temperature range. According to Fritzen-Freire et al. (2012), weight losses between 30 and 100 °C could be attributed to moisture loss. In the case of MD, there was a stage from ~270 to ~350 °C which resulted in a weight loss of ~66%. AB exhibited a large weight loss (~56%) at a lower onset temperature (~160–350 °C). These could be attributed to the decomposition of long molecular amine units of proteins and depolymerization of polysaccharides (Tavares & Zapata Noreña, 2019). According to Fritzen-Freire et al. (2012), the degradation of inulin occurred between 213 °C and 223 °C. The weight that remained above 350 °C was ~30 and 40%

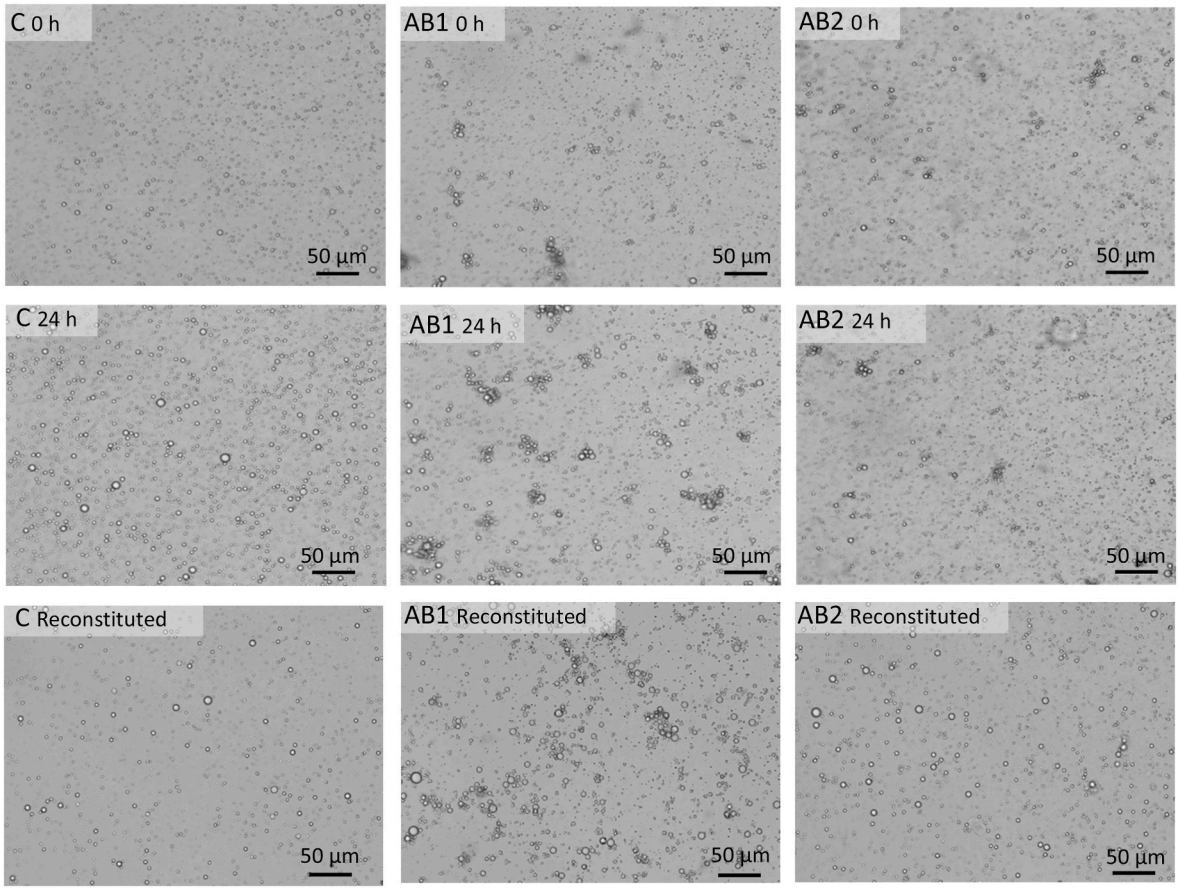

Fig. 3. Micrographs of emulsions control (C), AB1, and AB2 obtained at time 0 h and after 24 h.

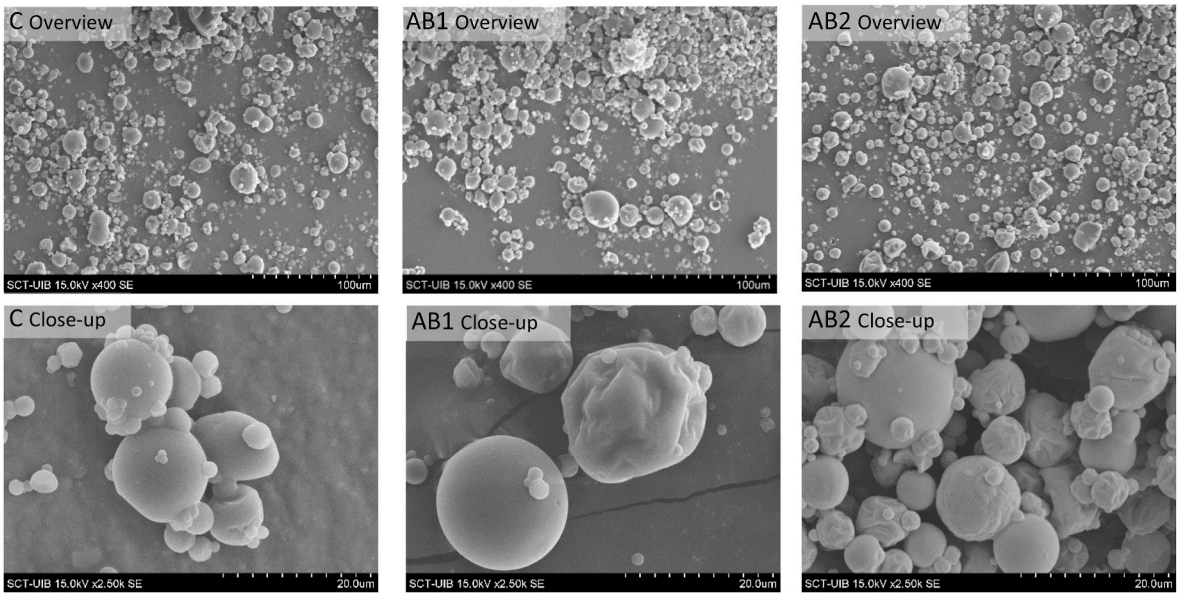

Fig. 4. Scanning electron microscope micrographs of control (C), AB1, and AB2 powders (spray dried emulsions).

of the initial weight for MD and AB, respectively. The presence of inorganic compounds could explain the higher remaining weight of AB. Regarding the microcapsules (Fig. 6B), the addition of AB affected the TGA curves decreasing the onset temperature in the stage with the largest weight loss. Thus, this stage started at ~280 °C in C and ~210 °C in AB1 and AB2. However, the weight loss was higher in this stage for C (~70%) than for AB1 and AB2 (~60%).

According to the DSC thermograms (Supplementary 2), the Tg of MD was 93.54 ± 3.91 °C, similar to that reported by Descamps et al. (2013) (~90 °C at 4% moisture content). Regarding AB, some low molecular weight components as free monosaccharides might affect the Tg (Table 2) which was significantly ($p < 0.05$) lower than the value for

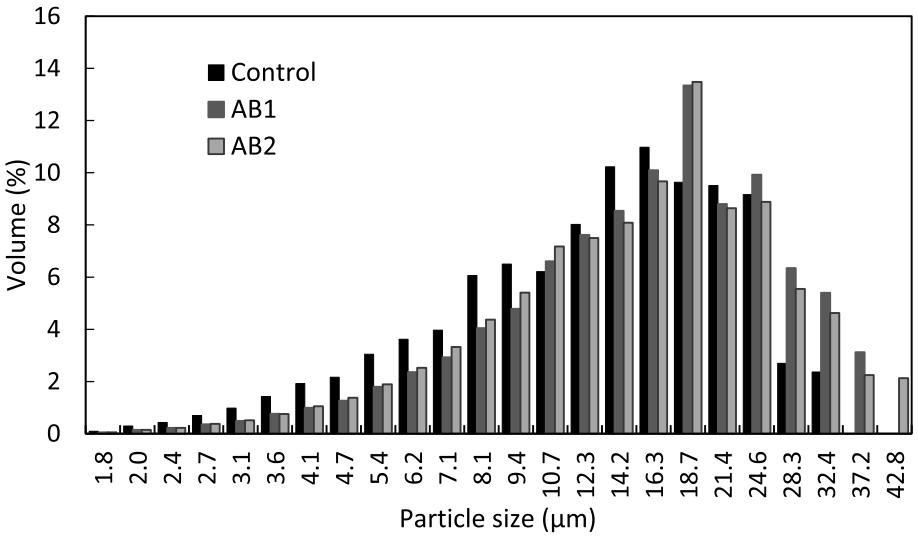

Fig. 5. The particle size distribution of control (C), AB1, and AB2 microcapsules.

Table 3
Characteristics of control (C), AB1, and AB2 powders (dried emulsions).

	C			AB1			AB2		
Particle size									
d_{10} (μm)	5.25	±	0.52^{b}	6.75	±	0.31^{a}	6.56	±	0.18^{a}
d_{50} (μm)	13.17	±	0.61^{b}	15.45	±	0.95^{a}	14.95	±	0.89^{a}
d_{90} (μm)	22.87	±	1.26^{b}	27.21	±	0.72^{a}	28.27	±	0.99^{a}
Span	1.34	±	0.20^{a}	1.33	±	0.05^{a}	1.46	±	0.17^{a}
Encapsulation efficiency (%)	65.72	±	1.97^{b}	66.56	±	1.00^{b}	78.90	±	0.99^{a}
Moisture content (g/100 g dm)	2.70	±	0.09^{a}	2.17	±	0.12^{b}	2.29	±	0.19^{b}
Water activity	0.170	±	0.002^{a}	0.119	±	0.003^{b}	0.127	±	0.010^{b}
Hygroscopicity (%)	11.35	±	0.52^{a}	11.93	±	0.52^{a}	11.49	±	0.33^{a}
Solubility (%)	91.95	±	3.97^{a}	84.80	±	0.17^{b}	83.04	±	1.62^{b}
CIELab Colour coordinates									
L*	97.74	±	0.21^{a}	82.31	±	0.50^{b}	76.81	±	0.24^{c}
a*	−0.04	±	0.01^{c}	1.53	±	0.08^{b}	1.81	±	0.19^{a}
b*	0.77	±	0.06^{c}	13.51	±	0.37^{b}	16.72	±	0.09^{a}
ΔE				20.07	±	0.62^{b}	26.38	±	0.29^{a}
ρ_b (kg/m^3)	568	±	7^{a}	564	±	11^{a}	586	±	20^{a}
ρ_t (kg/m^3)	609	±	5^{a}	602	±	4^{a}	626	±	16^{a}
ρ (kg/m^3)	1065	±	87^{a}	1018	±	35^{a}	1030	±	100^{a}
Porosity	0.43	±	0.05^{a}	0.41	±	0.03^{a}	0.39	±	0.02^{a}
Flow properties									
HR	1.07	±	0.01^{a}	1.07	±	0.02^{a}	1.07	±	0.04^{a}
CCI (%)	6.71	±	0.54^{a}	6.34	±	0.52^{a}	6.41	±	0.54^{a}
Tg (°C)	91.20	±	1.77^{a}	89.44	±	1.69^{a}	87.93	±	3.31^{a}
SA	4.75	±	0.33^{a}	4.35	±	0.38^{a}	3.00	±	0.25^{b}

An average of at least three replicates is reported. Different letters in the same row indicate significant ($p < 0.05$) differences.

MD. AB did not significantly ($p > 0.05$) affect Tg for the microcapsules (Table 3). The Tg was high for all the samples meaning that below ~85 °C no undesired caking would be expected in storage with low RH (Balasubramanian et al., 2016).

3.4. Oxidative stability

The SA of conjugated dienes in the stripped sunflower oil was 2.45 ± 0.01. The SA of the oil in the microcapsules (Table 3) was significantly ($p < 0.05$) higher than that of the stripped oil. Thus, there was an initial oxidation process of the oil during emulsification and spray drying. This has been previously reported by Serfert et al. (2009) who observed an increase of hydroperoxide content in fish oil after emulsification and Hernández et al. (2016) who encapsulated sunflower oil with MD and observed an increase of SA after spray drying. These authors explained that this was a result of the oxygen content in the emulsion and the exposure of the oil droplet to a hot air current during spray drying. Interestingly, the SA value for AB2 was significantly ($p < 0.05$) lower than those of both AB1 and C.

Fig. 7 shows the evolution of SA of the encapsulated oil during controlled storage. A rapid increase of SA was observed in the oil of C at the beginning of the storage, thus SA increased till 49 after 15 days. From this moment onwards, it decreased to 25 and then slowly increased till ~56 after 3 months. Hernández et al. (2016) also observed a sharp increase of SA in encapsulated sunflower oil with MD in the first days of storage (60 °C, 50% RH); explaining that this was probably due to the oxidation of non-encapsulated oil. Conjugated dienes are primary oxidation products and they do not remain when oxidation moves to further stages (Schaich, 2016). This explains the decrease of SA observed in C from day 15. The further increase observed from day 28 might indicate that the encapsulated oil also started autoxidation. For AB1 and AB2, the oil oxidation was initially slower compared with C. From day 28, SA increased significantly ($p < 0.05$) faster in AB1 than in AB2.

PUFAs autoxidation begins as hydrogen is abstracted from their

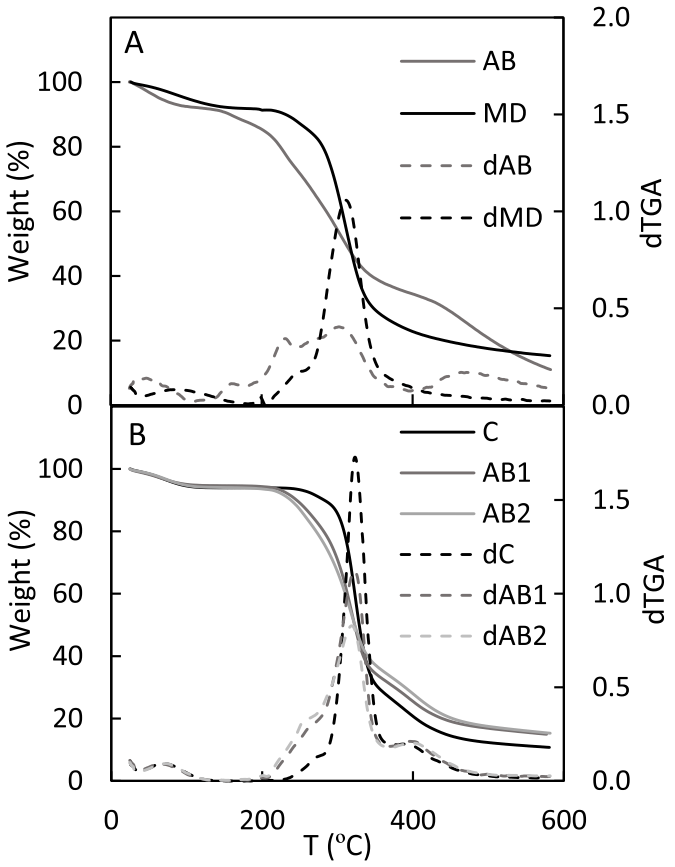

Fig. 6. Thermogravimetric analyses and its derivates (dashed lines) (dTGA) of A) maltodextrin (MD) and artichoke bracts (AB) and B) Control (C), AB1, and AB2 microcapsules.

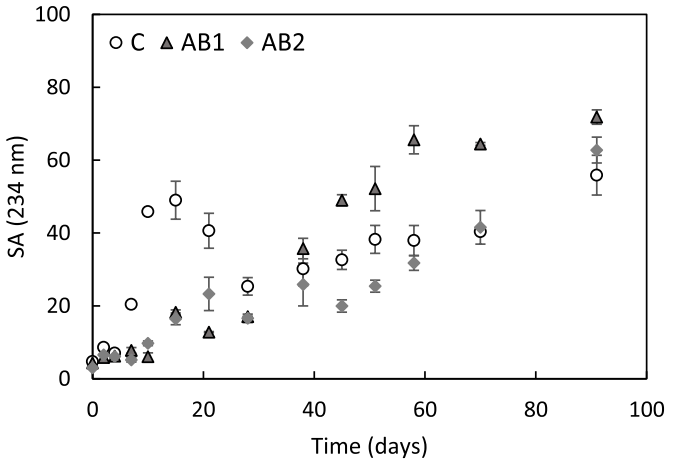

Fig. 7. Oxidation stability of oil at 35 °C and 50% RH in terms of specific absorbance (SA) at 234 nm, as indicative of the evolution of conjugated dienes.

structure, which could be prevented by adding compounds with more readily abstractable hydrogens (Garner, 1988). Phenolic compounds are known for their ability to donate hydrogen, their presence in AB probably delayed the oil oxidation (Mathew et al., 2015).

The main fatty acids of the stripped sunflower oil and oil in the microcapsules are shown in Fig. 8. This composition did not significantly ($p > 0.05$) change after spray drying. However, after 90 days of storage, the linoleic acid proportion decreased by 21, 23, and 24% in C, AB1 and AB2. This agrees with the increase of SA during storage since conjugated

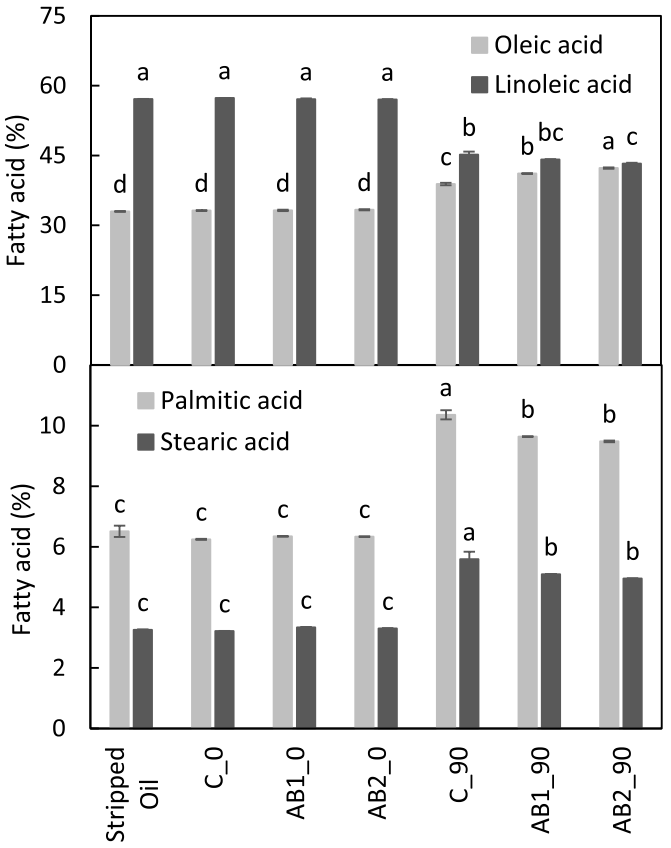

Fig. 8. Fatty acid composition of initial stripped oil (Strip. oil), of oil after spray drying (0 days of storage): C_0, AB1_0 and AB2_0 and after 90 days of storage: C_90, AB1_90, AB2_90. Different letters on the top of the bars of the same fatty acid indicate significant ($p < 0.05$) differences among the samples.

dienes are originated from PUFAs (as linoleic acid) oxidation (Schaich, 2016). The rest of the fatty acids increased by 17, 24, and 27% in C, AB1, and AB2 (oleic acid), 66, 52, and 50% (palmitic acid) and 74, 53, and 50% (stearic acid). Thus, the oil in C showed the highest stearic and palmitic acid increments. The increase of saturated fatty acids and the decrease of PUFAs have been used as an indicator of oils degradation (Aniołowska & Kita, 2015; Li et al., 2017). This suggests that the oil within C was more degraded after 90 days than the oil of powders containing AB. This agrees with the SA results, which indicate that the initiation stage of oxidation started earlier in C oil.

The better oxidative stability of the oil encapsulated in AB2 could be due to the higher presence of antioxidant compound coming from AB in this powder. Moreover, it could also be related to the higher ($p < 0.05$) encapsulation efficiency observed in AB2 (section 3.3) comparing with C and AB1. In addition, the C powder presented the highest moisture content and aw, this could have made the oil encapsulated in this powder more susceptible to oxidation (Aksoylu & GünçErgönül, 2017). Other parameters, such as the porosity, the hygroscopicity, the density, the flow properties, or the Tg of the powders, were no significantly different ($p > 0.05$) among the samples meaning that they did not cause the differences observed in the oxidative stability of the encapsulated oil.

However, even when the antioxidant compounds of AB were able to delay oil oxidation, they were probably degraded after 90 days, as is demonstrated by the high SA figures and the linoleic acid decrease. Shi et al. (2020) observed that after 3 months of storage (40 °C) of powders containing tuna oil encapsulated with green tea leaves, the catechins of the leaves suffered losses of up to 52%.

4. Conclusions

According to our results, using 2% AB in O/W emulsion, significantly ($p < 0.05$) increased the apparent viscosity to ~124 mPa s ($\gamma = 53\ s^{-1}$) leading to good stability against coalescence and flocculation (for 24 h). The powder obtained after spray drying the emulsions with AB exhibited similar hygroscopicity, density, porosity, flow properties, and Tg than the control. The oil encapsulation efficiency was significantly ($p < 0.05$) higher in AB2 (79%) comparing with the control (66%). Significantly ($p < 0.05$) lower moisture content and solubility in water, besides perceptible colour changes, were observed in powders containing AB. Moreover, AB2 showed lower oxidation indicators content after spray drying and for 2 months of controlled storage than the control, this was probably a result of the higher encapsulation efficiency of the oil in AB2 as well as of the presence of antioxidant molecules in AB. In conclusion, artichoke bracts are a healthy alternative to synthetic emulsifiers and could be successfully combined with common wall materials for lipids microencapsulation.

CRediT authorship contribution statement

Mónica Umaña: Methodology, Investigation, Data curation, Validation, Writing – original draft. **Paweł Wawrzyniak:** Conceptualization, Writing – review & editing. **Carmen Rosselló:** Resources, Writing – review & editing, Supervision. **Beatriz Llavata:** Validation, Visualization. **Susana Simal:** Conceptualization, Formal analysis, Writing – review & editing, Supervision, Funding acquisition, Project administration.

Declaration of competing interest

The authors declare that they have no known competing financial interests or personal relationships that could have appeared to influence the work reported in this paper.

Acknowledgments

The authors acknowledge the financial support of the National Institute of Research and Agri-Food Technology (INIA), ERDF funds EU, and the Spanish research agency (AEI) (RTA2015-00060-C04-03 and RTA2015-00060-C04-02), and the AEI (PID2019-106148RR-C43 AEI 10.13039/501100011033 and PID2019-106148RRC42 AEI 10.13039/501100011033 projects); and the Ministry of Science Innovation and Universities (MCIU) for the research fellowship (FPU15/03040) and the mobility aid (EST17/00152). We would also like to thank Dr. Fernando Hierro, Trinidad García, Josep Agustí Pablo Cànaves, and Dr. Joan Cifre Bauzà, from the "Serveis Cientificotècnics" of the University of the Balearic Islands for their assistance with SEM and optical microscopy, gas chromatography, HPLC and TGA and DSC respectively.

Appendix A. Supplementary data

Supplementary data to this article can be found online at https://doi.org/10.1016/j.lwt.2021.112146.

References

Aksoylu, Z., & Günç Ergönül, P. (2017). A review on encapsulation of oils. *Celal Bayar Üniversitesi Fen Bilimleri Dergisi, 13*(2), 293–309. https://doi.org/10.18466/cbayarfbe.313358

Almela, L., Rodríguez, T., Roca, M. J., Martínez, D., & Fernández-López, J. A. (2005). Quantity and quality of proteins in artichoke by-products (Cynara scolymus L.). *Acta Horticulturae, 681*, 505–510. https://doi.org/10.17660/ActaHortic.2005.681.70

Aniołowska, M., & Kita, A. (2015). The effect of type of oil and degree of degradation on glycidyl esters content during the frying of French fries. *JAOCS, Journal of the American Oil Chemists' Society, 92*(11–12), 1621–1631. https://doi.org/10.1007/s11746-015-2715-3

Aoac. (1997). *Official methods of analysis of AOAC International*.

AOCS. (2006). *Official method Ce 2-66*.

Balasubramanian, S., Devi, A., Singh, K. K., Bosco, S. J. D., & Mohite, A. M. (2016). Application of glass transition in food processing. In *Critical reviews in food science and nutrition* (Vol. 56, pp. 919–936). Taylor and Francis Inc. https://doi.org/10.1080/10408398.2012.734343. Issue 6.

Berton-Carabin, C., & Schroën, K. (2019). Towards new food emulsions: Designing the interface and beyond. *Current Opinion in Food Science, 27*, 74–81. https://doi.org/10.1016/J.COFS.2019.06.006

Can Karaca, A., Low, N. H., & Nickerson, M. T. (2015). Potential use of plant proteins in the microencapsulation of lipophilic materials in foods. *Trends in Food Science & Technology, 42*(1), 5–12. https://doi.org/10.1016/J.TIFS.2014.11.002

Carneiro, H. C. F., Tonon, R. V., Grosso, C. R. F., & Hubinger, M. D. (2013). Encapsulation efficiency and oxidative stability of flaxseed oil microencapsulated by spray drying using different combinations of wall materials. *Journal of Food Engineering, 115*(4), 443–451. https://doi.org/10.1016/J.JFOODENG.2012.03.033

Coimbra, M. a, Delgadillo, I., Waldron, K. W., & Selvendran, R. R. (1996). Isolation and analysis of cell wall polymers from olive pulp. *Modern Methods of Plant Analysis, 17*, 19–44. https://doi.org/10.1007/978-3-642-60989-3_2

Costa, A. M. M., Nunes, J. C., Lima, B. N. B., Pedrosa, C., Calado, V., Torres, A. G., & Pierucci, A. P. T. R. (2015). Effective stabilization of CLA by microencapsulation in pea protein. *Food Chemistry, 168*, 157–166. https://doi.org/10.1016/j.foodchem.2014.07.016

Descamps, N., Palzer, S., Roos, Y. H., & Fitzpatrick, J. J. (2013). Glass transition and flowability/caking behaviour of maltodextrin DE 21. *Journal of Food Engineering, 119*(4), 809–813. https://doi.org/10.1016/J.JFOODENG.2013.06.045

Di Giorgio, L., Salgado, P. R., & Mauri, A. N. (2019). Encapsulation of fish oil in soybean protein particles by emulsification and spray drying. *Food Hydrocolloids, 87*, 891–901. https://doi.org/10.1016/j.foodhyd.2018.09.024

Dickinson, E. (2009). Hydrocolloids and emulsion stability. In *Handbook of hydrocolloids* (2nd ed., pp. 23–49). Elsevier Inc. https://doi.org/10.1533/9781845695873.23.

Dodds, E. D., McCoy, M. R., Rea, L. D., & Kennish, J. M. (2005). Gas chromatographic quantification of fatty acid methyl esters: Flame ionization detection vs. electron impact mass spectrometry. *Lipids, 40*(4), 419–428. https://doi.org/10.1007/s11745-006-1399-8

Domingo, C. S., Rojas, A. M., Fissore, E. N., & Gerschenson, L. N. (2019). Rheological behavior of soluble dietary fiber fractions isolated from artichoke residues. *European Food Research and Technology, 245*(6), 1239–1249. https://doi.org/10.1007/s00217-019-03242-y

Drusch, S. (2007). Sugar beet pectin: A novel emulsifying wall component for microencapsulation of lipophilic food ingredients by spray-drying. *Food Hydrocolloids, 21*(7), 1223–1228. https://doi.org/10.1016/j.foodhyd.2006.08.007

Edris, A. E., Kalemba, D., Adamiec, J., & Piątkowski, M. (2016). Microencapsulation of Nigella sativa oleoresin by spray drying for food and nutraceutical applications. *Food Chemistry, 204*, 326–333. https://doi.org/10.1016/J.FOODCHEM.2016.02.143

Eim, V. S., Simal, S., Rosselló, C., & Femenia, A. (2008). Effects of addition of carrot dietary fibre on the ripening process of a dry fermented sausage (sobrassada). *Meat Science, 80*(2), 173–182. https://doi.org/10.1016/J.MEATSCI.2007.11.017

Faustino, M., Veiga, M., Sousa, P., Costa, E. M., Silva, S., & Pintado, M. (2019). Agro-food byproducts as a new source of natural food additives. In *Molecules* (Vol. 24)MDPI AG. https://doi.org/10.3390/molecules24061056. Issue 6.

Fioramonti, S. A., Stepanic, E. M., Tibaldo, A. M., Pavón, Y. L., & Santiago, L. G. (2019). Spray dried flaxseed oil powdered microcapsules obtained using milk whey proteins-alginate double layer emulsions. *Food Research International, 119*, 931–940. https://doi.org/10.1016/j.foodres.2018.10.079

Franck, A. (2002). Technological functionality of inulin and oligofructose. *British Journal of Nutrition, 87*(S2), S287–S291. https://doi.org/10.1079/bjn/2002550

Fritzen-Freire, C. B., Prudêncio, E. S., Amboni, R. D. M. C., Pinto, S. S., Negrão-Murakami, A. N., & Murakami, F. S. (2012). Microencapsulation of bifidobacteria by spray drying in the presence of prebiotics. *Food Research International, 45*(1), 306–312. https://doi.org/10.1016/j.foodres.2011.09.020

Gallotti, F., Lavelli, V., & Turchiuli, C. (2020). Application of Pleurotus ostreatus β-glucans for oil–in–water emulsions encapsulation in powder. *Food Hydrocolloids, 105*, 105841. https://doi.org/10.1016/j.foodhyd.2020.105841

Garner, H. (1988). Oxygen radical chemistry OF polyunsaturated fatty acids. *Free Radical Biology Do Medicine, 7*, 65–86. https://doi.org/10.1177/1461444810365020

Gaurav, S. (2003). In G. Sharma, & R. Bala (Eds.), *Digital color imaging notebook*.

GEA Niro Method No. (2005). *A 10 a*. GEA Niro Analytical Methods.

Gharibzahedi, S. M. T., George, S., Greiner, R., Estevinho, B. N., Frutos Fernández, M. J., McClements, D. J., & Roohinejad, S. (2018). New trends in the microencapsulation of functional fatty acid-rich oils using transglutaminase catalyzed crosslinking. *Comprehensive Reviews in Food Science and Food Safety, 17*(2), 274–289. https://doi.org/10.1111/1541-4337.12324

Gharsallaoui, A., Roudaut, G., Chambin, O., Voilley, A., & Saurel, R. (2007). Applications of spray-drying in microencapsulation of food ingredients: An overview. *Food Research International, 40*(9), 1107–1121. https://doi.org/10.1016/J.FOODRES.2007.07.004

Gharsallaoui, A., Saurel, R., Chambin, O., Cases, E., Voilley, A., & Cayot, P. (2010). Utilisation of pectin coating to enhance spray-dry stability of pea protein-stabilised oil-in-water emulsions. *Food Chemistry, 122*(2), 447–454. https://doi.org/10.1016/j.foodchem.2009.04.017

He, K., Li, Q., Li, Y., Li, B., & Liu, S. (2020). Water-insoluble dietary fibers from bamboo shoot used as plant food particles for the stabilization of O/W Pickering emulsion. *Food Chemistry, 310*, 125925. https://doi.org/10.1016/j.foodchem.2019.125925

Hernández Sanchez, M. D. R., Cuvelier, M. E., & Turchiuli, C. (2015). Design of liquid emulsions to structure spray dried particles. *Journal of Food Engineering, 167*, 99–105. https://doi.org/10.1016/j.jfoodeng.2015.07.036

Hernández Sánchez, M. del R., Cuvelier, M. E., & Turchiuli, C. (2016). Effect of α-tocopherol on oxidative stability of oil during spray drying and storage of dried emulsions. *Food Research International, 88*, 32–41. https://doi.org/10.1016/j.foodres.2016.04.035

Hosseini, A., Jafari, S. M., Mirzaei, H., Asghari, A., & Akhavan, S. (2015). Application of image processing to assess emulsion stability and emulsification properties of Arabic gum. *Carbohydrate Polymers, 126*, 1–8. https://doi.org/10.1016/j.carbpol.2015.03.020

Huc-Mathis, D., Almeida, G., & Michon, C. (2021). Pickering emulsions based on food byproducts: A comprehensive study of soluble and insoluble contents. *Journal of Colloid and Interface Science, 581*, 226–237. https://doi.org/10.1016/j.jcis.2020.07.078

Jenkins, P., & Snowden, M. (1996). Depletion flocculation in colloidal dispersions. *Advances in Colloid and Interface Science, 68*(1–3), 57–96. https://doi.org/10.1016/s0001-8686(96)90046-9

Kim, E. H., Chen, X. D., & Pearce, D. (2005). Melting characteristics of fat present on the surface of industrial spray-dried dairy powders. *Colloids and Surfaces B: Biointerfaces, 42*(1), 1–8. https://doi.org/10.1016/J.COLSURFB.2005.01.004

Le Tan, H., Tran, T., Ton, T. M., Tran, T. T., Huynh, T., Nguyen, T. N., Quang, S. P., & Le, V. (2017). Combination of whey protein and carbohydrate for microencapsulation of pumpkin (Cucurbita spp.) seed oil by spray-drying. *International Food Research Journal*. https://www.researchgate.net/publication/317869679_Combination_of_whey_protein_and_carbohydrate_for_microencapsulation_of_pumpkin_Cucurbita_spp_seed_oil_by_spray-drying.

Li, X., Li, J., Wang, Y., Cao, P., & Liu, Y. (2017). Effects of frying oils' fatty acids profile on the formation of polar lipids components and their retention in French fries over deep-frying process. *Food Chemistry, 237*, 98–105. https://doi.org/10.1016/j.foodchem.2017.05.100

Linke, A., Weiss, J., & Kohlus, R. (2020). Factors determining the surface oil concentration of encapsulated lipid particles: Impact of the emulsion oil droplet size. *European Food Research and Technology, 246*(10), 1933–1943. https://doi.org/10.1007/s00217-020-03545-5

Locali, A. R., Gonçalves Cattelan, M., of pink pepper essential oil: P. of spray-dried pectin/SPI double-layer versus S. single-layer stabilized emulsions, Nicoletti, V. R. (2019). Microencapsulation of pink pepper essential oil: Properties of spray-dried pectin/SPI double-layer versus SPI single-layer stabilized emulsions. *Colloids and Surfaces A: Physicochemical and Engineering Aspects, 581*, 123806. https://doi.org/10.1016/j.colsurfa.2019.123806

Low, L. E., Siva, S. P., Ho, Y. K., Chan, E. S., & Tey, B. T. (2020). Recent advances of characterization techniques for the formation, physical properties and stability of Pickering emulsion. In *Advances in colloid and interface science* (Vol. 277, p. 102117). Elsevier B.V. https://doi.org/10.1016/j.cis.2020.102117.

Marson, G. V., Saturno, R. P., Comunian, T. A., Consoli, L., Machado, M. T. da C., & Hubinger, M. D. (2020). Maillard conjugates from spent brewer's yeast by-product as an innovative encapsulating material. *Food Research International, 136*, 109365. https://doi.org/10.1016/j.foodres.2020.109365

Massel, V., Fang, Y., & Corredig, M. (2021). Pectin nanoemulsions in multiple emulsions: Stability and encapsulation efficiency. *Food Research International, 139*, 109950. https://doi.org/10.1016/j.foodres.2020.109950

Mathew, S., Abraham, T. E., & Zakaria, Z. A. (2015). Reactivity of phenolic compounds towards free radicals under in vitro conditions. *Journal of Food Science & Technology, 52*(9), 5790–5798. https://doi.org/10.1007/s13197-014-1704-0

Mena-García, A., Rodríguez-Sánchez, S., Ruiz-Matute, A. I., & Sanz, M. L. (2020). Exploitation of artichoke byproducts to obtain bioactive extracts enriched in inositols and caffeoylquinic acids by Microwave Assisted Extraction. *Journal of Chromatography A, 1613*, 460703. https://doi.org/10.1016/j.chroma.2019.460703

de Mendiburu, F. (2016). *Agricolae: Statistical Procedures for agricultural research (R package version 1.2-4)*.

Mohammed, N. K., Tan, C. P., Manap, Y. A., Muhialdin, B. J., & Hussin, A. S. M. (2020). Spray drying for the encapsulation of oils—a review. In *Molecules* (Vol. 25)MDPI AG. https://doi.org/10.3390/molecules25173873. Issue 17.

Multari, S., Marsol-Vall, A., Heponiemi, P., Suomela, J. P., & Yang, B. (2019). Changes in the volatile profile, fatty acid composition and other markers of lipid oxidation of six different vegetable oils during short-term deep-frying. *Food Research International, 122*, 318–329. https://doi.org/10.1016/j.foodres.2019.04.026

Nasri, R., Taktak, W., Hamdi, M., Ben Amor, N., Kabadou, A., Li, S., & Nasri, M. (2020). Sardinelle protein isolate as a novel material for oil microencapsulation: Novel alternative for fish by-products valorisation. *Materials Science and Engineering: C, 116*, 111164. https://doi.org/10.1016/j.msec.2020.111164

Ng, M. L., & Sulaiman, R. (2018). Development of beetroot (Beta vulgaris) powder using foam mat drying. *Lebensmittel-Wissenschaft und -Technologie- Food Science and Technology, 88*, 80–86. https://doi.org/10.1016/j.lwt.2017.08.032

Pandino, G., Lombardo, S., Mauromicale, G., & Williamson, G. (2011). Profile of polyphenols and phenolic acids in bracts and receptacles of globe artichoke (Cynara cardunculus var. scolymus) germplasm. *Journal of Food Composition and Analysis, 24*(2), 148–153. https://doi.org/10.1016/j.jfca.2010.04.010

Pieczykolan, E., & Kurek, M. A. (2019). Use of guar gum, gum Arabic, pectin, beta-glucan and inulin for microencapsulation of anthocyanins from chokeberry. *International Journal of Biological Macromolecules, 129*, 665–671. https://doi.org/10.1016/J.IJBIOMAC.2019.02.073

Premi, M., & Sharma, H. K. (2017). Effect of different combinations of maltodextrin, gum Arabic and whey protein concentrate on the encapsulation behavior and oxidative stability of spray dried drumstick (Moringa oleifera) oil. *International Journal of Biological Macromolecules, 105*, 1232–1240. https://doi.org/10.1016/J.IJBIOMAC.2017.07.160

Qi, J., ru, S., wen, L., Zeng, W., qi, Liao, J., & song. (2020). Citrus fiber for the stabilization of O/W emulsion through combination of Pickering effect and fiber-based network. *Food Chemistry, 343*, 128523. https://doi.org/10.1016/j.foodchem.2020.128523

R Core Team. (2017a). *Foreign: Read data stored by minitab, S, SAS, SPSS, stata, systat, weka, dBase*.

R Core Team. (2017b). *R: A language and environment for statistical computing*. R Foundation for Statistical Computing.

Rasband, W. (2020). *Image, 1.52a*.

Rascón, M. P., Beristain, C. I., García, H. S., & Salgado, M. A. (2011). Carotenoid retention and storage stability of spray-dried encapsulated paprika oleoresin using gum Arabic and Soy protein isolate as wall materials. *Lebensmittel-Wissenschaft und -Technologie- Food Science and Technology, 44*(2), 549–557. https://doi.org/10.1016/j.lwt.2010.08.021

Ré, M. I. (1998). Microencapulsation of spray drying. *Drying Technology, 16*(6), 1195–1236. https://doi.org/10.1080/07373939808917460

Rodríguez, Ó., Ortuño, C., Simal, S., Benedito, J., Femenia, A., & Rosselló, C. (2014). Acoustically assisted supercritical CO2 extraction of cocoa butter: Effects on kinetics and quality. *The Journal of Supercritical Fluids, 94*, 30–37. https://doi.org/10.1016/j.supflu.2014.06.017

Ruiz-Aceituno, L., García-Sarrió, M. J., Alonso-Rodriguez, B., Ramos, L., & Sanz, M. L. (2016). Extraction of bioactive carbohydrates from artichoke (Cynara scolymus L.) external bracts using microwave assisted extraction and pressurized liquid extraction. *Food Chemistry, 196*, 1156–1162. https://doi.org/10.1016/j.foodchem.2015.10.046

Ruiz-Cano, D., Pérez-Llamas, F., Frutos, M. J., Arnao, M. B., Espinosa, C., López-Jiménez, J.Á., Castillo, J., & Zamora, S. (2014). Chemical and functional properties of the different by-products of artichoke (Cynara scolymus L.) from industrial canning processing. *Food Chemistry, 160*, 134–140. https://doi.org/10.1016/j.foodchem.2014.03.091

Saengkanuk, A., Nuchadomrong, S., Jogloy, S., Patanothai, A., & Srijaranai, S. (2011). A simplified spectrophotometric method for the determination of inulin in Jerusalem artichoke (Helianthus tuberosus L.) tubers. *European Food Research and Technology, 233*(4), 609–616. https://doi.org/10.1007/s00217-011-1552-3

Schaich, K. M. (2016). Analysis of lipid and protein oxidation in fats, oils, and foods. In *Oxidative stability and shelf life of foods containing oils and fats* (pp. 1–131). Elsevier Inc. https://doi.org/10.1016/B978-1-63067-056-6.00001-X.

Schuster, S., Bernewitz, R., Guthausen, G., Zapp, J., Greiner, A. M., Köhler, K., & Schuchmann, H. P. (2012). Analysis of W 1/O/W 2 double emulsions with CLSM: Statistical image processing for droplet size distribution. *Chemical Engineering Science, 81*, 84–90. https://doi.org/10.1016/j.ces.2012.06.059

Serfert, Y., Drusch, S., Schmidt-Hansberg, B., Kind, M., & Schwarz, K. (2009). Process engineering parameters and type of n-octenylsuccinate-derivatised starch affect oxidative stability of microencapsulated long chain polyunsaturated fatty acids. *Journal of Food Engineering, 95*(3), 386–392. https://doi.org/10.1016/J.JFOODENG.2009.05.021

Shi, M., Ying, D. Y., Hlaing, M. M., Ye, J. H., Sanguansri, L., & Augustin, M. A. (2020). Oxidative stability of spray dried matcha-tuna oil powders. *Food Research International, 132*, 109050. https://doi.org/10.1016/j.foodres.2020.109050

Tavares, L., & Zapata Noreña, C. P. (2019). Encapsulation of garlic extract using complex coacervation with whey protein isolate and chitosan as wall materials followed by spray drying. *Food Hydrocolloids, 89*, 360–369. https://doi.org/10.1016/J.FOODHYD.2018.10.052

Timilsena, Y. P., Wang, B., Adhikari, R., & Adhikari, B. (2017). Advances in microencapsulation of polyunsaturated fatty acids (PUFAs)-rich plant oils using complex coacervation: A review. In *Food hydrocolloids* (Vol. 69, pp. 369–381). Elsevier B.V. https://doi.org/10.1016/j.foodhyd.2017.03.007.

Tonon, R. V., Grosso, C. R. F., & Hubinger, M. D. (2011). Influence of emulsion composition and inlet air temperature on the microencapsulation of flaxseed oil by spray drying. *Food Research International, 44*(1), 282–289. https://doi.org/10.1016/J.FOODRES.2010.10.018

Tze, N. L., Han, C. P., Yusof, Y. A., Ling, C. N., Talib, R. A., Taip, F. S., & Aziz, M. G. (2012). Physicochemical and nutritional properties of spray-dried pitaya fruit powder as natural colorant. *Food Science and Biotechnology, 21*(3), 675–682. https://doi.org/10.1007/s10068-012-0088-z

Umaña, M., Eim, V., Garau, C., Rosselló, C., & Simal, S. (2020). Ultrasound-assisted extraction of ergosterol and antioxidant components from mushroom by-products and the attainment of a β-glucan rich residue. *Food Chemistry, 332*, 127390. https://doi.org/10.1016/j.foodchem.2020.127390

Umaña, M., Turchiuli, C., Rosselló, C., & Simal, S. (2021). Addition of a mushroom by-product in oil-in-water emulsions for the microencapsulation of sunflower oil by spray drying. *Food Chemistry, 343*, 128429. https://doi.org/10.1016/j.foodchem.2020.128429

Vallespir, F., Rodríguez, Ó., Eim, V. S., Rosselló, C., & Simal, S. (2018). Freezing pre-treatments on the intensification of the drying process of vegetables with different structures. *Journal of Food Engineering, 239*, 83–91. https://doi.org/10.1016/J.JFOODENG.2018.07.008

Vallespir, F., Rodríguez, Ó., Eim, V. S., Rosselló, C., & Simal, S. (2019). Effects of freezing treatments before convective drying on quality parameters: Vegetables with different microstructures. *Journal of Food Engineering, 249*, 15–24. https://doi.org/10.1016/j.jfoodeng.2019.01.006

Villanueva-Suárez, M. J., Mateos-Aparicio, I., Pérez-Cózar, M. L., Yokoyama, W., & Redondo-Cuenca, A. (2019). Hypolipidemic effects of dietary fibre from an artichoke by-product in Syrian hamsters. *Journal of Functional Foods, 56*, 156–162. https://doi.org/10.1016/J.JFF.2019.03.013

Wang, M., Simon, J. E., Aviles, I. F., He, K., Zheng, Q. Y., & Tadmor, Y. (2003). Analysis of antioxidative phenolic compounds in artichoke (Cynara scolymus L.). *Journal of Agricultural and Food Chemistry, 51*(3), 601–608. https://doi.org/10.1021/jf020792b

Whitby, C. P., Scarborough, H., & Ngothai, Y. (2017). Drying oil-in-water Pickering emulsions to make redispersible powders. *Advanced Powder Technology, 28*(11), 2940–2946. https://doi.org/10.1016/j.apt.2017.09.001

Xu, W., Xiong, Y., Li, Z., Luo, D., Wang, Z., Sun, Y., & Shah, B. R. (2020). Stability, microstructural and rheological properties of complex prebiotic emulsion stabilized by sodium caseinate with inulin and konjac glucomannan. *Food Hydrocolloids, 105*. https://doi.org/10.1016/j.foodhyd.2020.105772

Ye, Q., Georges, N., & Selomulya, C. (2018). Microencapsulation of active ingredients in functional foods: From research stage to commercial food products. In *Trends in food science and Technology* (Vol. 78, pp. 167–179). Elsevier Ltd. https://doi.org/10.1016/j.tifs.2018.05.025.

Zeaiter, Z., Regonesi, M. E., Cavini, S., Labra, M., Sello, G., & Di Gennaro, P. (2019). Extraction and characterization of inulin-type fructans from artichoke wastes and their effect on the growth of intestinal bacteria associated with health. *BioMed Research International, 2019*. https://doi.org/10.1155/2019/1083952

Zhu, Y., Ren, X., Bao, Y., Li, S., Peng, Z., Zhang, Y., & Zhou, G. (2020). Emulsification of oil-in-water emulsions with eggplant (Solanum melongena L.). *Journal of Colloid and Interface Science, 563*, 17–26. https://doi.org/10.1016/j.jcis.2019.12.055

Zotarelli, M. F., da Silva, V. M., Durigon, A., Hubinger, M. D., & Laurindo, J. B. (2017). Production of mango powder by spray drying and cast-tape drying. *Powder Technology, 305*, 447–454. https://doi.org/10.1016/J.POWTEC.2016.10.027